AFRRI TR84-8

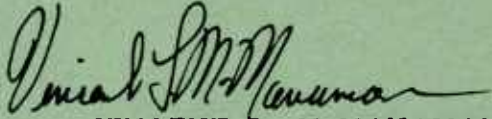# Paired ion chamber constants for fission gamma-neutron fields
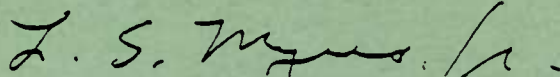
G. H. Zeman
K. P. Ferlic

DEFENSE NUCLEAR AGENCY
ARMED FORCES RADIOBIOLOGY RESEARCH INSTITUTE
BETHESDA, MARYLAND 20814-5145

REVIEWED AND APPROVED

VINCENT L. McMANAMAN
CDR, MSC, USN
Chairman
Radiation Sciences Department

LAWRENCE S. MYERS, Ph.D.
Scientific Director

BOBBY R. ADCOCK
COL, MS, USA
Director

REPORT DOCUMENTATION PAGE

1a. REPORT SECURITY CLASSIFICATION	1b. RESTRICTIVE MARKINGS
UNCLASSIFIED	

2a. SECURITY CLASSIFICATION AUTHORITY	3. DISTRIBUTION/AVAILABILITY OF REPORT
	Approved for public release; distribution unlimited.
2b. DECLASSIFICATION/DOWNGRADING SCHEDULE	

4. PERFORMING ORGANIZATION REPORT NUMBER(S)	5. MONITORING ORGANIZATION REPORT NUMBER(S)
AFRRI TR84-8	

6a. NAME OF PERFORMING ORGANIZATION	6b. OFFICE SYMBOL (If applicable)	7a. NAME OF MONITORING ORGANIZATION
Armed Forces Radiobiology Research Institute	AFRRI	

6c. ADDRESS (City, State and ZIP Code)	7b. ADDRESS (City, State and ZIP Code)
Defense Nuclear Agency Bethesda, Maryland 20814-5145	

8a. NAME OF FUNDING/SPONSORING ORGANIZATION	8b. OFFICE SYMBOL (If applicable)	9. PROCUREMENT INSTRUMENT IDENTIFICATION NUMBER
Defense Nuclear Agency	DNA	

8c. ADDRESS (City, State and ZIP Code)	10. SOURCE OF FUNDING NOS.			
	PROGRAM ELEMENT NO.	PROJECT NO.	TASK NO.	WORK UNIT NO.
Washington, DC 20305	NWED QAXM			MJ 00137

11. TITLE (Include Security Classification)
(See cover)

12. PERSONAL AUTHOR(S)
Zeman, G. H.

13a. TYPE OF REPORT	13b. TIME COVERED	14. DATE OF REPORT (Yr., Mo., Day)	15. PAGE COUNT
Technical	FROM _____ TO _____	December 1984	34

16. SUPPLEMENTARY NOTATION

17.	COSATI CODES		18. SUBJECT TERMS (Continue on reverse if necessary and identify by block number)
FIELD	GROUP	SUB. GR.	

19. ABSTRACT (Continue on reverse if necessary and identify by block number)

Paired ionization chamber constants are calculated for the 50 cm^3 spherical ionization chambers used in dosimetry of the AFRRI TRIGA reactor. The calculations include the most recently available information on energy spectra for neutron and gamma radiation present in AFRRI reactor exposure rooms, as well as for kerma factors and W-values of neutrons. The constant k_T, which expresses neutron sensitivity of the 50 cm^3 tissue equivalent (TE) ion chamber filled with TE gas, ranged from 0.92 to 0.96 among the 18 different neutron spectra for which calculations were done. The constant k_U, which expresses neutron sensitivity of the 50 cm^3 graphite ion chamber filled with CO_2, ranged from 0.07 to 0.11 among the same spectra. The constant h_T, which expresses gamma sensitivity of the TE/TE ion chamber, was taken to be unity for all spectra. The constant h_U, which expresses gamma sensitivity of the C/CO_2 ion chamber, was 0.99 ± 0.01 (range) for all spectra. These calculations will serve as the basis for future dosimetry with the 50 cm^3 ion chambers at the AFRRI TRIGA reactor.

20. DISTRIBUTION/AVAILABILITY OF ABSTRACT	21. ABSTRACT SECURITY CLASSIFICATION	
UNCLASSIFIED/UNLIMITED ☐ SAME AS RPT. ☒ OTIC USERS ☐	UNCLASSIFIED	

22a. NAME OF RESPONSIBLE INDIVIDUAL	22b. TELEPHONE NUMBER (Include Area Code)	22c. OFFICE SYMBOL
J. A. Van Deusen	(202) 295-3536	ADMG

DD FORM 1473, 83 APR   EDITION OF 1 JAN 73 IS OBSOLETE.

CONTENTS

INTRODUCTION

Paired ionization chambers used for the dosimetry of mixed gamma-neutron radiation consist of tissue-equivalent (TE) chambers and nonhydrogenous chambers. TE chambers respond to both neutron and gamma radiation, and their readings are closely related to the total dose. Nonhydrogenous chambers are relatively insensitive to neutron radiation; they primarily record the gamma dose. This report presents detailed derivations of the characteristics of response for two ionization chambers used for mixed gamma-neutron dosimetry: an A-150 plastic chamber operated with TE gas (TE/TE) and a graphite chamber filled with carbon dioxide (C/CO_2). (The compositions of A-150 plastic- and methane-based TE gas are given in reference 1.) These spherical 50-cm^3 ion chambers were originally described by Lynn (2) and Sayeg (3), and are diagrammed in Figure 1. They served as the backbone of AFRRI mixed-field dosimetry measurements since 1965 (e.g., references 4-6).
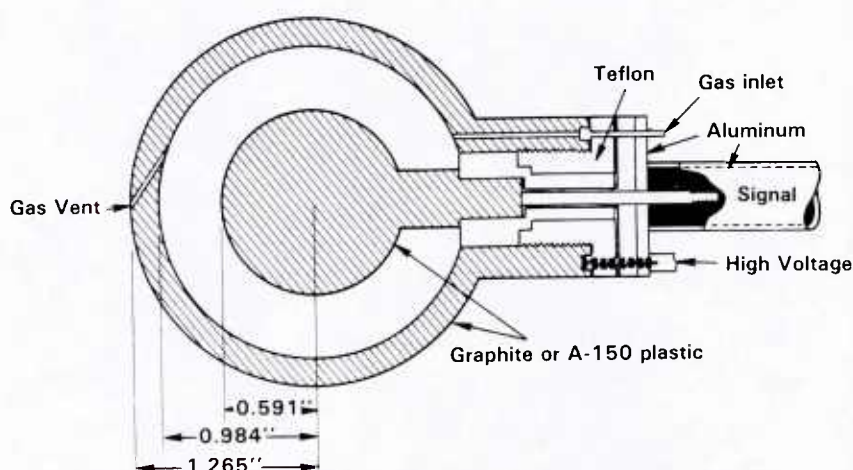

Figure 1. AFRRI spherical 50 cm^3 ion chambers

The recent availability of spectral information for both neutron and gamma-ray energy (7, 8) for the AFRRI TRIGA reactor has prompted the present review of the response characteristics of the 50-cm^3 chamber. This information enables calculation of both the neutron and gamma-ray sensitivities of the paired chambers, in accordance with currently accepted neutron dosimetry protocols (1, 9, 10). Moreover, the physical constants involved in calculating neutron dosimetry, such as kerma factors and W-values, are known now with much greater certainty (11-13). Thus, reevaluation of the response characteristics of the ion chamber is necessary, to serve as a basis for future work and to clarify the accuracy of previous estimates of these parameters.

Theory

The response of paired ion chambers to mixed neutron-gamma radiation is expressed as follows (1):

$$R_T = k_T D_N + h_T D_G \qquad \text{(Eq 1)}$$

$$R_U = k_U D_N + h_U D_G \qquad \text{(Eq 2)}$$

where D_N and D_G represent the respective neutron and gamma components of the total dose deposited in tissue. R_T and R_U represent the readings of TE/TE and C/CO_2 ion chambers, respectively, divided by the cobalt-60 calibration factor (coulomb per rad) for each chamber. The k's and h's, known as the paired chamber constants, represent the sensitivity of each chamber (subscript T for TE/TE, U for C/CO_2) to neutron and gamma radiation (k for neutron, h for gamma), relative to its sensitivity to cobalt-60 radiation.

4

Values of the paired chamber constants depend on the energy spectra of the neutron and gamma radiation, according to the following:

$$k_{T,U} = \frac{\overline{W_C}}{\overline{W_N}} \cdot (Smg)_C \frac{(\mu_{en}/\rho)_t/(\mu_{en}/\rho)m\ _C}{(K_t/K_g)_N} \qquad \text{(Eq 3)}$$

$$h_{T,U} = \frac{\overline{W_C}}{\overline{W_G}} \cdot \frac{(Smg)_C}{(Smg)_G} \frac{(\mu_{en}/\rho)_t/(\mu_{en}/\rho)m\ _C}{(\mu_{en}/\rho)_t/(\mu_{en}/\rho)m\ _G} \qquad \text{(Eq 4)}$$

where

C	=	Subscript for cobalt-60 calibration field
N	=	Subscript for neutron spectrum to be measured
G	=	Subscript for gamma spectrum to be measured
m	=	Subscript for ion chamber wall material
g	=	Subscript for ion chamber gas
t	=	Subscript for tissue, i.e., ICRU muscle (1)
W	=	Average energy to produce an ion pair in TE or CO_2 gas
(Smg)	=	Ratio of electron mass–stopping powers of ion–chamber wall material to that of ion–chamber gas material
(μ_{en}/ρ)	=	Mass energy transfer coefficient for gamma radiation
K	=	Average kerma factor of neutron spectrum

That the above equations apply to the AFRRI 50-cm^3 paired ion chambers is based on two assumptions: (a) Ionizations in chamber gas caused by neutrons are entirely due to neutron interactions that occur in the gas, not the wall. This is because the ion chambers are relatively large, compared to the short range of recoil nuclei generated in neutron interactions in chamber walls. This is especially true of the low-energy neutrons encountered in fission neutron spectra. For C/CO$_2$ chambers, Markewicz and Pszona (14) showed that even a 1-cm^3 ion chamber satisfied this condition for neutrons with energies up to 15 MeV. For TE/TE chambers, recoil protons from chamber wall material have longer ranges than do recoil C nuclei in the C/CO$_2$ chamber, but the kerma factors for A-150 plastic and TE gas are almost equal to each other (1), and the W-value for wall recoils is nearly equal to the W-value for gas recoils (12). (b) The above equation for h_T and h_U uses Fano's Theorem, based on the nearly matching elemental composition of wall and gas in the TE/TE chamber, and on the similarity in atomic numbers of carbon and oxygen, together with the almost unity value of (Smg) (see below) for the C/CO$_2$ chamber.

METHODS

Cobalt-60 Calibration Field

Dosimetric parameters for the cobalt-60 calibration field are given in Table 1, with appropriate references.

6

Table 1. Dosimetric Parameters for Cobalt-60 Calibration Field

Parameter	Value	Reference
$(\mu_{en}/\rho)_t(\mu_{en}/\rho)_m$		
TE/TE	1.001	Broerse et al. (1981)
C/CO$_2$	1.126	ORNL (1975)
$(Smg)_C$		
TE/TE	1.000	Broerse et al. (1981)
C/CO$_2$	1.009	AAPM (1980)
W_C		
TE/TE	29.3 JC^{-1}	Broerse et al. (1981)
C/CO$_2$	33.0 JC^{-1}	ICRU (1979)

Gamma Fields of the Reactor

Gamma fields of the reactor include photons distributed in energy from 10 keV to 10 MeV (8). The average gamma energies of these spectra range from 0.67 to 1.8 MeV (15). For such spectra, the average energy to produce an ion pair, W, can be taken to be the same as for cobalt-60 gamma rays (16).

For the TE/TE ion chamber, the tissue equivalence of the material of the chamber wall and the close match in elemental composition of the wall and gas allow use of the same stopping power ratio and mass energy transfer coefficient ratio for reactor gamma fields as for cobalt-60 gamma rays. Thus, for the TE/TE ion chamber, the paired chamber constant h_T can be taken to be unity for all reactor gamma fields, as is done for higher energy neutron beams (9, 10).

7

For the C/CO_2 ion chamber, the energy dependence of both (Smg) and μ_{en}/ρ must be accounted for to properly evaluate h_U for energy spectra of reactor gamma rays. This was completed in an earlier report (15) for the mass energy transfer coefficients; results are duplicated in Table 2. Because the gas-to-wall ratio (Smg) for mass-stopping power is a slowly varying function of electron (or gamma-ray) energy, an approximate method was used to arrive at suitable values for reactor gamma fields. For each reactor configuration, the average gamma-ray energy was used to derive an average energy for Compton recoil electrons (17). This average energy was referred to tables of electron collision mass-stopping power (18), to derive the ratios of stopping power shown in Table 2. These ratios varied between 1.002 and 1.022, compared to 1.009 for cobalt-60 gamma rays. The lowest ratios were for the configurations with the largest populations of low-energy scattered photons, i.e., the configurations near the back walls of the exposure rooms.

Reactor Neutron Fields

The ratios of spectrum-averaged kerma factors for tissue to those for both TE gas and CO_2 were derived in an earlier report (15), and are listed in Table 3 for reference. Neutron W-values for TE gas and CO_2 have been the subject of several recent reports (12, 13) demonstrating a complicated dependence on energy for both gases. Published data on neutron W-values is incomplete, particularly for low-energy neutrons (below 0.5 MeV), and the remaining uncertainties in W have been recognized as one of the major sources of uncertainty in dosimetry of neutron radiation (1). The W-values used in the present report are given in Table 4

for the energy groupings in which reactor neutron spectra were tabulated. Detailed discussion of these values is presented in the Appendix. Averaging of the neutron-W values over the reactor neutron spectra was arrived at by using computer program SPT (15), as described in the Appendix. Resulting spectrum-averaged W-values for all reactor configurations are given in Table 3.

Table 2. Dosimetric Parameters for Graphite-CO_2 Ion Chamber in Gamma Ray Fields of Reactor

Room	Distance to Core (cm)	Configuration*	Average Energy (MeV)	$(Smg)_G$	$(\mu_{en}/\rho)_t/(\mu_{en}/\rho)_{mG}$
1	50	Unshielded	1.16	1.012	1.128
	100	Unshielded	1.15	1.012	1.130
	200	Unshielded	1.05	1.010	1.132
	300	Unshielded	0.91	1.007	1.134
	400	Unshielded	0.78	1.004	1.139
	500	Unshielded	0.67	1.002	1.149
2	50	Unshielded	1.18	1.012	1.129
	100	Unshielded	1.13	1.011	1.129
	200	Unshielded	0.95	1.008	1.135
	300	Unshielded	0.76	1.004	1.142
2	30	Pneumatic tubes	0.83	1.005	1.138
1	100	5" H_2O	1.04	1.009	1.131
	100	12" H_2O	0.95	1.009	1.137
	100	2" Pb	1.65	1.008	1.128
	100	2" Pb and exercise wheel	1.36	1.022	1.131
	100	6" Pb	0.92	1.016	1.142
	100	6" Pb and cave	1.80	1.007	1.132
	100	6" Pb and cylinder phantom	1.13	1.011	1.133

*For complete description of reactor configuration, see references 7 and 8.

Table 3. Dosimetric Parameters for Neutron Fields of Reactor

Room	Distance to Core (cm)	Configuration	Average Neutron Energy (MeV)	W_N (eV) TE$_{gas}$	W_N (eV) CO$_2$	K_t/K_g TE$_{gas}$	K_t/K_g CO$_2$
1	50	Unshielded	1.46	31.7	44.3	0.980	9.57
	100	Unshielded	1.49	31.7	44.2	0.979	9.50
	200	Unshielded	1.32	31.6	44.4	0.983	9.62
	300	Unshielded	1.16	31.7	44.5	0.981	9.89
	400	Unshielded	1.11	31.8	44.6	0.986	9.78
	500	Unshielded	0.89	31.8	45.2	0.984	9.84
2	50	Unshielded	1.35	31.7	44.1	0.979	9.59
	100	Unshielded	1.32	31.7	44.4	0.986	9.66
	200	Unshielded	1.11	31.7	44.2	0.984	9.68
	300	Unshielded	0.93	31.7	44.8	0.981	9.81
2	30	Pneumatic tubes	0.88	31.8	44.9	0.982	10.21
1	100	5" H$_2$O	1.99	31.5	42.9	0.979	9.26
	100	12" H$_2$O	3.71	31.2	40.7	0.983	8.49
	100	2" Pb	1.58	31.7	45.0	0.986	9.67
	100	2" Pb and exercise wheel	1.05	31.8	45.7	0.984	9.92
	100	6" Pb	0.96	32.0	47.1	0.983	10.18
	100	6" Pb and cave	0.68	32.0	49.0	0.986	10.38
	100	6" Pb and cylinder phantom	0.55	32.3	47.7	0.986	11.00

Table 4. Group W Values of the Neutron Spectrum

Energy Group	Group Upper Energy (MeV)	W(eV) TE Gas	W(eV) CO$_2$
1	19.6	31.0	35.5
2	16.9	31.0	35.9
3	14.9	31.0	36.1
4	14.2	31.0	36.1
5	13.8	31.0	36.4
6	12.8	31.0	36.7
7	12.2	31.0	37.0
8	11.1	31.1	37.5
9	10.0	31.1	37.9
10	9.0	31.1	38.4
11	8.2	31.2	39.0
12	7.4	31.0	38.7
13	6.4	31.1	40.1
14	5.0	31.1	39.3
15	4.7	31.2	40.2
16	4.1	31.5	42.4
17	3.0	31.3	41.7
18	2.4	31.0	41.7
19	2.3	31.3	43.8
20	1.8	31.5	47.1
21	1.1	32.9	49.0
22	0.55	32.4	61.3
23	0.16	33.4	75.2
24	0.11	33.6	84.1
25	0.052	34.6	98.2
26	0.025	36.0	107.7
27	0.022	38.3	
28	0.010	51.0	
29	0.0034	146.2	
30	0.0011		

RESULTS

Before presenting the derived paired-chamber constants for the various reactor configurations, each ion chamber's energy response curves for both gamma and neutron radiation should be examined. The neutron results (shown in Figure 2) were obtained using the neutron-W values of Table 4 and the neutron-kerma factors (11) for individual spectrum-energy groups. Figure 2 also shows the response curve calculated by Markewicz and Pszona (14), using Monte Carlo techniques for a large C/CO_2 chamber for neutrons above 1 MeV. This curve compares closely with the results derived here. The range of reported C/CO_2 k_U values summarized by Mijnheer (19) for 15-MeV neutrons also compares favorably with the present results. Measured TE/TE (1 cm^3) and C/CO_2 (2 cm^3) ion-chamber responses for neutrons over 1 MeV reported by Waterman et al. (20) are also shown in Figure 2. For the TE/TE chamber, the present results agree well with the measured responses for neutrons below 10 MeV. The lower C/CO_2 k_U values measured for neutrons above 5 MeV is surprising, because for smaller ion chambers (such as those used by Waterman et al.), one would expect k_U values to be higher than for large chambers (14). Possible explanations for the low k_T and k_U values measured at high-neutron energies are discussed by Waterman et al. (20).

At the time of this writing, for neutron energies below 1 MeV, there exists no published calculation or measurements of k_T or k_U to compare with the present results. This is due to the emphasis on high-energy neutron beams in the recent literature, particularly for clinical radiotherapy applications.
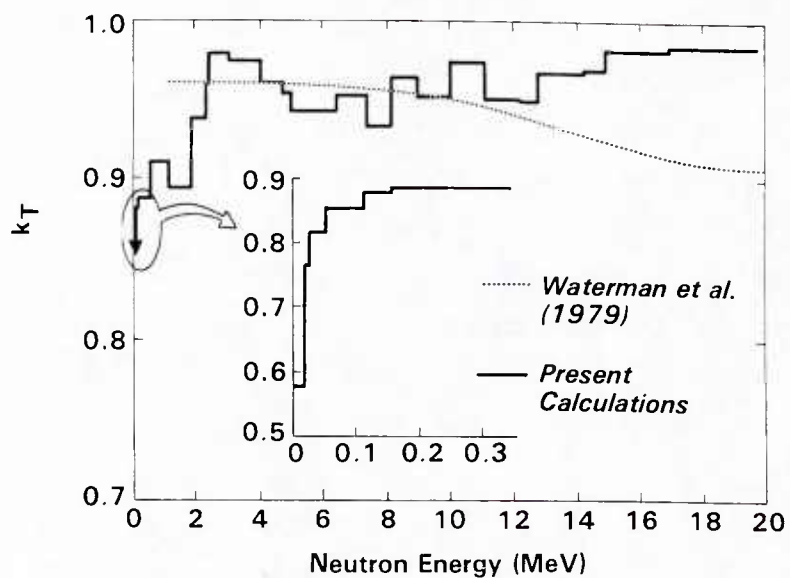
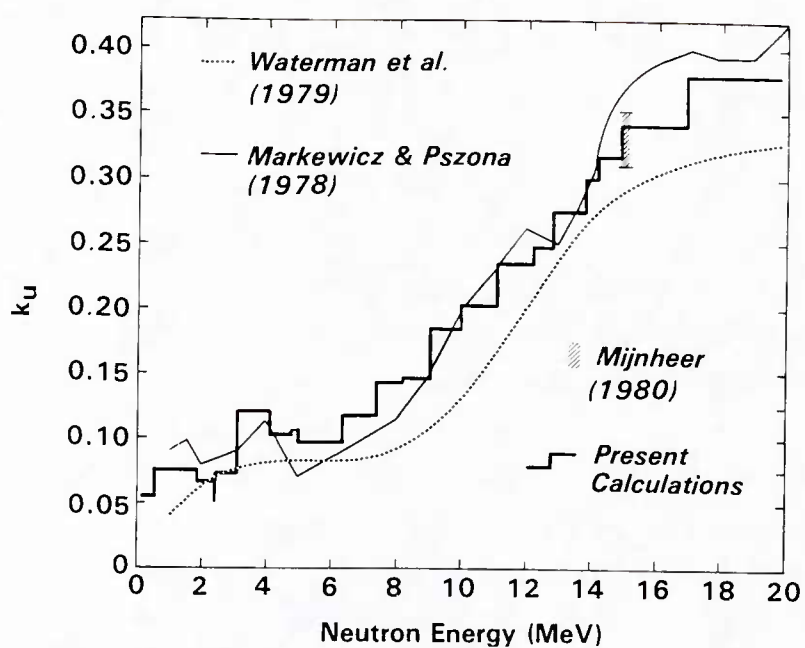Figure 2a. Neutron sensitivity of TE ion chamber

Figure 2b. Neutron sensitivity of graphite ion chamber

The calculated photon energy response of the C/CO_2 ion chamber is shown in Figure 3. (Recall that the photon energy response of the TE/TE ion chamber was taken to be unity, based on the tissue equivalence of

A-150 plastic and methane-based TE gas.) The decrease in h_U for the C/CO_2 ion chamber at low photon energies occurs mainly because the graphite atomic number is lower than that of tissue, thus causing fewer photoelectric interactions. At high photon energies (over 2 MeV), the increased values of h_U are due mainly to the energy dependence of (Smg). Recall that (Smg) was obtained by an approximation technique (see Methods), but the relatively low flux of reactor gamma rays above 2.2 MeV minimizes errors in the photon response due to (Smg) uncertainties.
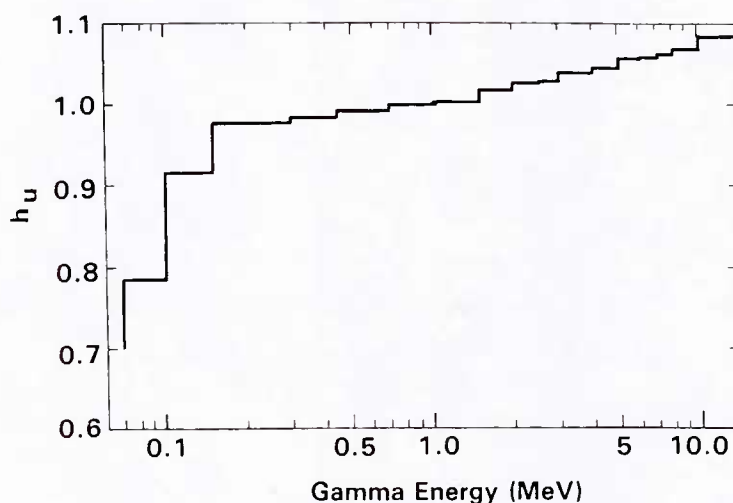

Figure 3. Gamma sensitivity of C/CO_2 ion chamber

Paired ionization chamber constants evaluated for TRIGA reactor gamma-neutron spectra are given in Table 5. The precision of displayed results is probably greater than warranted by the accuracy of the calculations, but it is useful for demonstrating the spectral dependence of the constants. These results show a clear separation in k_T and k_U values between the water-shielded reactor configurations and all other configurations. This occurs because of the higher average

energies of water-shielded neutron spectra. For h_U, a single value was found to apply within $\pm$ 1% for all spectra.

Table 5. Paired Ion Chamber Constants for AFRRI Reactor Configurations

Room	Distance to Core (cm)	Configuration	TE/TE k_T	C/CO$_2$ k_U	C/CO$_2$ h_U
1	50	Unshielded	0.944	0.0862	0.995
	100	Unshielded	0.945	0.0870	0.993
	200	Unshielded	0.944	0.0855	0.994
	300	Unshielded	0.943	0.0830	0.995
	400	Unshielded	0.935	0.0837	0.994
	500	Unshielded	0.937	0.0821	0.987
2	50	Unshielded	0.945	0.0864	0.994
	100	Unshielded	0.938	0.0852	0.995
	200	Unshielded	0.940	0.0854	0.993
	300	Unshielded	0.943	0.0831	0.991
2	30	Pneumatic tubes	0.939	0.0797	0.993
1	100	5" H$_2$O	0.951	0.0919	0.996
	100	12" H$_2$O	0.956	0.1057	0.990
	100	2" Pb	0.938	0.0839	0.999
	100	2" Pb & exercise wheel	0.937	0.0806	0.983
	100	6" Pb	0.933	0.0762	0.979
	100	6" Pb & cave	0.930	0.0718	0.997
	100	6" Pb & cyl phantom	0.921	0.0696	0.992

*h_T = 1.000 for all configurations.

DISCUSSION

This work has incorporated recently reported AFRRI TRIGA reactor gamma-neutron energy spectra together with up-to-date estimates of pertinent kerma factors and W-values, to evaluate the energy response characteristics of AFRRI 50-cm^3 paired ionization chambers. This derivation of the paired-chamber constants shall serve as the basis for future dosimetric measurements with these ion chambers; it can also elucidate the

validity of estimates of these constants used in the past. Verification of the derived constants by experimentation has not been considered in the present work, but it will be the subject of future research.

ACKNOWLEDGMENT

APPENDIX. VALUES OF NEUTRON-W FOR METHANE-BASED

TE GAS AND CO_2

W is defined as the quotient of E divided by N, where N is the mean number of ion pairs formed when the initial kinetic energy, E, of a charged particle is completely dissipated in the gas. For neutron radiation, it is necessary to consider the energy deposited by several different types of charged particles interacting in the gas. Following Goodman and Coyne (12), the W-value for neutrons of energy, E_n, is defined as follows:

$$W_N(E_N) = \frac{\sum\limits_{j} K_j(E_N)}{\sum\limits_{j} N_j(E_N)} \qquad \text{(Eq A-1)}$$

Where $N_j(E_n)$ is the number of ions produced by secondary charged particles of type j, which deposit kerma $K_j(E_n)$. $N_j(E_n)$ and $K_j(E_n)$ are calculated as follows:

$$N_j(E_N) = \int_0^{E_{max\,j}} \frac{n_j(E,E_N)E\,dE}{W_j(E)} \qquad \text{(Eq A-2)}$$

$$K_j(E_N) = \int_0^{E_{max\,j}} n_j(E,E_N)E\,dE \qquad \text{(Eq A-3)}$$

where $n_j(E,E_n)$ represents the initial differential energy spectrum of charged particles of type j produced by unit neutron fluence of energy E_n, and $W_j(E)$ is the W-value for type j particles with initial energy E.

For neutrons with energies distributed over a spectrum, the above theory must be extended to define a spectrum-averaged neutron W-value, denoted $\overline{W}_N$, as follows:

$$\overline{W}_N = E_d/N_s \qquad \text{(Eq A-4)}$$

19

In the above equation, E_d is the energy deposited, and N_S is the total ions produced per unit fluence. E_d and N_S are determined as follows:

$$E_d = \int_0^\infty K(E_N)\phi(E_N)dE_N = \sum_{g=1}^{37} K_g\phi_g\Delta E_g \qquad \text{(Eq A-5)}$$

$$N_S = \int_0^\infty \frac{K(E_N)\phi(E_N)dE_N}{W_N(E_N)} = \sum_{g=1}^{37} \frac{K_g\phi_g\Delta Eg}{W_g} \qquad \text{(Eq A-6)}$$

where $K(E_n)$ represents the gas-kerma factor for neutrons of energy E_n, and K_g represents the gas-kerma factor for neutrons that are in group g. Then $\phi(E)$ and ϕ_g represent the neutron energy spectrum, with the sums extending over the 37 energy groups in the neutron spectral format of reference 21. To complete the sums in the above equations, it is necessary to use average W_n values for each energy group (denoted by W_g). These are derived by averaging W_n between the upper E_U and lower E_L energies of each group, as follows:

$$W_g = \frac{\int_{E_L}^{E_u} K(E_N)\phi(E_N)dE_N}{\int_{E_L}^{E_u} \frac{K(E_N)\phi(E_N)dE_N}{W_N(E_N)}} = \frac{E_u - E_L}{\int_{E_L}^{E_u} \frac{dE_N}{W_N(E_N)}} \qquad \text{(Eq A-7)}$$

To obtain the right side of equation A-7, the neutron kerma factor $K(E_n)$ has been assumed to be proportional to E_n between neutron energies E_L and E_U, and $\phi(E_n)$

within each energy group has been assumed to have a dependence on 1/En.

TE GAS

The neutron W-values for TE gas of Goodman and Coyne (12) were used as the basis for the W-values of the spectrum groups shown in Table 4 for the energy range 19.6 MeV through 110 keV (energy spectrum groups 1 through 23). In the following, W is estimated for TE gas for neutrons with energies between 1 and 110 keV (groups 24 through 29). These estimates were based on the following assumptions:

a. The neutron kerma and the ionizations produced by neutrons in TE gas were considered to be due to recoil protons for the purpose of evaluating equations A-1, A-2, A-3, and A-7. This assumption was based on the fact that 94%-96% of the total kerma is, in fact, due to recoil protons in this range of neutron energy, and this percentage varies only slowly with neutron energy. The W-values calculated on the basis of this assumption were, in the end, corrected for the fraction of total kerma due to C, N, and O.

b. Goodman and Coyne's (12) empirical expression for W for protons in TE gas, which is valid for proton energies above 4 keV, was extrapolated to lower proton energies. This expression is $W_p = 29.28 \, (\ln E)^{-2} + 29.99$, where proton energy E is in units of keV and W_p is in units of eV. This assumption was needed because no experimental data existed on W for

protons (or neutrons) with energies below 4 keV. Extrapolation of this expression to lower energies had no physical justification, but no viable alternative was available.

c. Recoil protons with energies below 1 keV were assumed to produce no ionizations. Thus, the lower integration limit of equation A-2 for N_j is set at 1 keV.

Based on the above assumptions, the initial differential energy spectrum $n_p(E,E_n)$ for recoil protons is given by the spectrum that describes elastic scattering, namely $n_p(E,E_n) = \phi_p(E_n)/E_n$, where $\phi_p(E_n)$ represents the number of recoil protons arising from elastic scattering with neutrons of energy E_n. Equations A-2 and A-3 were evaluated as follows, with the subscript p denoting recoil protons:

$$K_p(E_N) = \tfrac{1}{2}E_N \phi_p(E_N) \qquad \text{(Eq A-8)}$$

$$N_p(E_N) = \frac{\phi_p(E_N)}{E_N} \int_{1\ keV}^{E_N} \frac{E\,dE}{29.28(\ln E)^{-2} + 29.99} \qquad \text{(Eq A-9)}$$

The above integral for $N_p(E_p)$ was evaluated numerically, and then approximated by the following expression with an error of 3% at 3 keV and less than 1% at $\geq$ 4 keV:

$$N_p(E_N) = \frac{\tfrac{1}{2}E_N \phi_p(E_N)}{30.86} \left\{ \frac{E_N - 1.82}{E_N + 0.76} \right\} \qquad \text{(Eq A-10)}$$

Using the results of equations A-8 and A-10 in equation A-1 gives the following for neutron W-values in TE gas:

$$W_N(E_N) = 30.86 \left\{ \frac{E_N + 0.76}{E_N - 1.82} \right\} \qquad \text{(Eq A-11)}$$

Recall that the above result does not include a correction for the fraction of the neutron kerma due to C, N, and O in TE gas. Equation A-11 was integrated following equation A-7, to arrive at neutron W_g-values for energy spectrum groups bounded by the lower and upper energies E_L and E_U, respectively.

$$W_g = \frac{30.86}{f} \; \frac{E_u - E_L}{E_u - E_L - 2.58 \ln \left\{ \dfrac{E_u + 0.76}{E_L + 0.76} \right\}} \qquad \text{(Eq A-12)}$$

In the above equation, the factor f represents the fraction of the total neutron kerma in TE gas that is due to recoil protons. (From reference 11, f is equal to 0.943 for energy group 23, 0.950 for 24, 0.956 for 25, 0.960 for 26 and 27, 0.962 for 28, and 0.960 for 29.) Equation A-12 yields the group Wg-values shown in Table 4 for spectrum groups 24 through 29.

For spectrum group 23 (110-160 keV), equation A-12 yields a W_g-value of 33.37 eV, which agrees within 2.4% with the value (32.60) estimated for group 23 from the results obtained by Goodman and Coyne (12). That the W_g-value derived here is higher than the Wg-value of Goodman and Coyne is probably due to the fact that the present calculation ignores ions produced by C, N, and

23

O recoils. For neutron energies below 100 keV, the percentage of ions produced by C, N, and O is even lower than in spectrum group 23, so errors due to this omission should be below 2% for spectrum groups 24 through 29.

Carbon Dioxide

Neutron W-values from three sources were used to arrive at the spectrum group W_g-values shown in Table 4: (a) Rubach and Bishell's (13) 19 data points between 0.45 and 14.0 MeV for infinitely large ion chambers (13). (Our graphite/CO_2 ion chamber is 50 cc volume.) (b) Dennis' data at 14.0, 14.7, and 15.5 MeV normalized to Rubach and Bishell's W_N-value at 14.0 MeV (22). (c) The estimated W-values for low-energy neutrons derived below. These W_N-values are plotted in Figure 4. Following equation A-7, interpolation between 1/W-values at discrete energies was used to evaluate the spectrum group Wg-values listed in Table 4.

W-values for low-energy neutrons (below 0.5 MeV) in CO_2 were estimated, based on the following assumptions:

a. Neutron interactions are dominated by elastic scattering with C and O. Initial differential energy spectra for C and O recoils are approximated by those for isotropic scattering in the center of mass system, namely: $\phi_c(E_n)/E_c(E_n)$ and $\phi_O(E_n)/E_O(E_n)$, respectively, where $E_c = 0.284\ E_n$ and $E_O = 0.221\ E_n$ are the maximum recoil energies.

b. Neutron W-values for recoil C and O ions in CO_2 are taken from the empirical expressions

24

of Rubach and Bischell (13). These are given below for recoil energies, E, expressed in MeV.

$$W_C = \begin{cases} 6.33 - 15.91 \ln E, & E < 0.080 \text{ MeV} \\ 38.26 - 3.26 \ln E, & 0.080 \leq E < 6 \text{ MeV} \end{cases}$$

(Eq A-13)

$$W_O = \begin{cases} 4.57 - 19.5 \ln E, & E < 0.1 \text{ MeV} \\ 45.59 - 2.99 \ln E, & 0.1 \leq E < 3.5 \text{ MeV} \end{cases}$$

Based on the assumption of isotropic elastic scattering, the kerma integrals (equation A-3) are evaluated as follows:

$$K_O = \tfrac{1}{2} E_O \phi_O(E_N)$$

$$K_C = \tfrac{1}{2} E_C \phi_C(E_N)$$

(Eq A-14)

Using Rubach and Bischell's (13) empirical expressions for W, equation 2 can be evaluated for the quantities $N_j(E_n)$. Consider first the C recoils.

$$N_C(E_N) = \begin{cases} \dfrac{\phi_C(E_N)}{E_C} \displaystyle\int_0^{E_C} \dfrac{E\,dE}{6.33 - 15.91 \ln E} & E < 0.080 \text{ MeV} \\[4ex] \dfrac{\phi_C(E_N)}{E_C} \left[\displaystyle\int_0^{0.08} \dfrac{E\,dE}{6.33 - 15.91 \ln E} + \displaystyle\int_{0.08}^{E_C} \dfrac{E\,dE}{38.26 - 3.26 \ln E} \right] & 0.080 < E < 6 \text{ MeV} \end{cases}$$

(Eq A-15)

25

Both the C and the O expressions for $N_j(E_n)$ involve integrals of the following form, which by a transformation of variables are reduced to the Exponential Integral $Ei(t)$, as below:

$$I = \int_a^b \frac{E\,dE}{a + \beta \ln E}$$

$$= \frac{\exp(-2a/\beta)}{-\beta} \int_{t(a)}^{t(b)} \frac{e^{-t}\,dt}{t} \quad \text{where } t = \frac{-2}{\beta}(a + \beta \ln E) \qquad \text{(Eq A-16)}$$

$$= \frac{\exp(-2a/\beta)}{-\beta} \left[Ei(t(a)) - Ei(t(b)) \right]$$

The integrals in the expressions for $N_c(E_n)$ of equation A-15 were evaluated for selected neutron energies, using tables of the Exponential Integral (23). Table 6 lists the results of these evaluations expressed in terms of the quantity $\Omega_c = (E_c{}^2/2I)$, which is effectively the W-value for a C-recoil spectrum, with maximum energy E_c. Similarly, the quantity $N_0(E_n)$ was evaluated for oxygen recoils, and terms $\Omega_0 = (E_0^2/2I)$ are listed in Table 6. Using these quantities, $N_c(E_n)$ and $N_0(E_n)$ can be expressed as follows:

$$N_c(E_N) = \tfrac{1}{2} E_c \phi_c(E_N)\, \Omega_c^{-1}$$

$$N_0(E_N) = \tfrac{1}{2} E_0 \phi_0(E_N)\, \Omega_0^{-1} \qquad \text{(Eq A-17)}$$

Combining equations A-14 and A-17 gives the W_n-values for CO_2 as

$$W_N = \frac{1 + f'}{\Omega_0^{-1} + f'\,\Omega_c^{-1}} \qquad \text{(Eq A-18)}$$

where the quantity f' is defined as:

$$f' = \frac{E_c \phi_c (E_N)}{E_o \phi_o (E_N)} \qquad \text{(Eq A-19)}$$

Thus f' represents the fraction of the neutron kerma in CO_2 due to C-recoils divided by the fraction due to O-recoils. This ratio is defined by the C and O kerma factors and the relative abundance of C and O in CO_2. Values of f' calculated from data in reference 11 are given in Table 6. The data in Table 6, together with equation A-18, formed the basis for the low-energy W_n-values (below 0.5 MeV), plotted in Figure 4.

Table 6. Quantities Used in Calculation of W for Low-Energy Neutrons in CO_2

E_n (keV)	E_c	Ω_c	E_o	Ω_o	f'
22	6.2	96.49	4.9	121.87	.79
25	7.1	93.70	5.5	118.69	.79
52	14.8	80.77	11.5	101.53	.76
110	31.2	68.66	24.3	86.25	.72
160	45.4	62.65	35.4	78.73	.48
445	126	48.31	98.3	58.38	.27
550	156	47.22	122	54.83	.80

*E_c and E_o are maximum energies of C and O recoil nuclei, respectively, arising from elastic scattering with neutrons of energy En. Ω_c and Ω_o are respective W-values for recoil C and O nuclei, with energies covering spectrum from zero to E_c and E_o, respectively. f' is fraction of neutron kerma in CO_2 due to C-recoils, divided by fraction due to O-recoils.
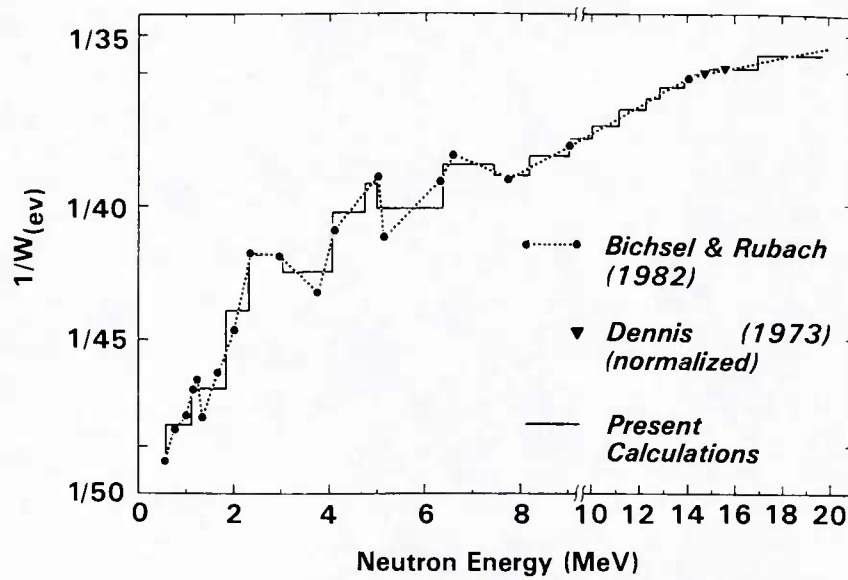
Figure 4. Neutron W values for CO_2

For 445-keV neutrons, the above derivation gave a W_n-value of 55.90 eV, which differed by 3.3% from the W_n-value published by Rubach and Bischell (13). At this energy, the neutron cross section for oxygen shows a strong resonance peak, and the assumption of isotropic elastic scattering is at its weakest.

REFERENCES

1. Neutron dosimetry for biology and medicine. ICRU Report 26, International Commission on Radiation Units and Measurements, Washington, DC, 1977.

2. Lynn, R. L. Tissue equivalent ionization chambers. In: Manual of Radiation Dosimetry Experiments. Contract Report CR65-4, Armed Forces Radiobiology Research Institute, Bethesda, Maryland, 1965.

3. Sayeg, J. A. Neutron and gamma dosimetry measurements at the AFRRI-DASA TRIGA reactor. Contract Report CR65-6, Armed Forces Radiobiology Research Institute, Bethesda, Maryland, 1965.

4. Verrelli, D. M. Dosimetry for neutron radiation studies in miniature pigs. Technical Note TN71-2, Armed Forces Radiobiology Research Institute, Bethesda, Maryland, 1971.

5. Shosa, D. W. Reactor dosimetry with paired miniature ionization chambers. Technical Note TN71-7, Armed Forces Radiobiology Research Institute, Bethesda, Maryland, 1971.

6. Zeman, G. H. Phantom dosimetry for TRIGA reactor irradiations in chair and wheel arrays. Technical Report TR84-6, Armed Forces Radiobiology Research Institute, Bethesda, Maryland, 1984.

7. Verbinski, V. V., Cassapakis, C. C., Hagan, W. K., Ferlic, K., and Daxon, E. Radiation field characterization for the AFRRI TRIGA reactor. Volume 1, Baseline Data and Evaluation of Calculational Data. DNA Report No. 5793F-1, Defense Nuclear Agency, Washington, DC, 1981.

8. Verbinski, V. V., Cassapakis, C. C., Hagan, W. K., Ferlic, K., and Daxon, E. Calculation of the neutron and gamma-ray environment in and around the TRIGA Reactor, Volume II. DNA Report No. 5793F-2, Defense Nuclear Agency, Washington, DC, 1981.

9. Broerse, J. J., Mijnheer, B. J., and Williams, J. R. European protocol for neutron dosimetry for external beam therapy. British Journal of Radiology 54: 882-898, 1981.

10. Protocol for neutron beam dosimetry. AAPM Report No. 7, American Association of Physicists in Medicine, American Institute of Physics, New York, 1980.

11. Zeman, G. H., and Bice, W. S., Jr. Kerma factors for use in 37-group neutron spectrum calculations. Technical Note TN83-3, Armed Forces Radiobiology Research Institute, Bethesda, Maryland, 1983.

12. Goodman, L. J., and Coyne, J. J. Wn and neutron kerma for methane-based tissue-equivalent gas. Radiation Research 82: 13-26, 1980.

13. Bichsel, H., and Rubach, A. Neutron dosimetry with spherical ionisation chambers. II. Basic physical data. Physics in Medicine and Biology 27: 1003-1013, 1982.

14. Markewicz, M., and Pszona, S. Theoretical characteristics of a graphite ionization chamber filled with carbon dioxide. Nuc. Inst. Meth. 153: 423-428, 1978.

15. Ferlic, K. P., and Zeman, G. H. Spectrum-averaged kerma factors for reactor dosimetry with paired ion chambers. Technical Report TR83-2, Armed Forces Radiobiology Research Institute, Bethesda, Maryland, 1983.

16. Average energy required to produce an ion pair. ICRU Report 31, International Commission on Radiation Units and Measurements, Washington, DC, 1979.

17. Evans, R. D. X-ray and gamma ray interactions. In: Radiation Dosimetry. Attix, F. H., and Roesch, W. C., eds. Academic Press, New York, 1968.

18. Berger, M. J., and Seltzer, S. M. Publication 1133, National Academy of Sciences—National Research Council, Washington, DC, 1964, p. 205.

19. Mijnheer, B. J. The relative neutron sensitivity, k_U, for non-hydrogenous detectors. In: Ion Chambers for Neutron Dosimetry, Broerse, J. J., ed. EUR 6782, Luxembourg:CEC, 1980.

20. Waterman, F. M., Kuchnir, F. T., and Skaggs, L. S. Energy dependence of the neutron sensitivity of $C-CO_2$, Mg-Ar, and TE-TE ionization chambers, Physics in Medicine and Biology 24: 721-733, 1979.

21. DLC-31/(DPL-1/FEWG1), 37-neutron, 21-gamma ray coupled, P3, multigroup library in ANISN Format. ORNL/TM-4840. Oak Ridge National Laboratories, Oak Ridge, Tennessee, 1975.

22. Dennis, J. A. Computed ionization and kerma values in neutron-irradiated gases. Physics in Medicine and Biology 18: 379-395, 1973.

23. Handbook of Mathematical Functions. Abramowitz, M., and Stegun, I. A., eds. National Bureau of Standards Applied Math Series 55, U.S. Department of Commerce, 1967.